Theory of induced quadrupolar order in tetragonal YbRu$_2$Ge$_2$

Tetsuya Takimoto and Peter Thalmeier

Max Planck Institute for Chemical Physics of Solids, Nöthnitzer Strasse 40, 01187 Dresden, Germany

(Received 17 August 2007; revised manuscript received 21 October 2007; published 8 January 2008)

The tetragonal compound YbRu$_2$Ge$_2$ exhibits a nonmagnetic transition at $T_0 = 10.2$ K and a magnetic transition at $T_1 = 6.5$ K in zero magnetic field. We present a model for this material based on a quasiquartet of Yb^{3+} crystalline electric field (CEF) states and discuss its mean-field solution. Taking into account the broadening of the specific heat jump at T_0 for magnetic field perpendicular to [001] and the decrease of T_0 with magnetic field parallel to [001], it is shown that ferroquadrupole order of either O$_2^2$- or O$_{xy}$-type are prime candidates for the nonmagnetic transition. Considering the matrix element of these quadrupole moments, we show that the lower CEF states of the level scheme consist of a Γ_6 and a Γ_7 doublet. This leads to induced type of O$_2^2$ and O$_{xy}$ quadrupolar order parameters. The quadrupolar order introduces exchange anisotropy for planar magnetic moments. This causes a spin-flop transition at low fields perpendicular [001] which explains the observed metamagnetism. We also obtain a good explanation for the temperature dependence of magnetic susceptibility and specific heat for fields both parallel and perpendicular to the [001] direction.

I. INTRODUCTION

It is well known that some *f*-electron systems show multipole ordering. The phenomenon has attracted much attention, since features of multipole order are quite different from usual magnetic order. As a typical case, CeB$_6$ shows a kind of antiferroquadrupole ordering at 3.4 K, whose transition temperature increases with increasing magnetic field.[1–3] For transition in NpO$_2$, an octupole ordering is proposed due to experimental results of resonant x-ray scattering[4–6] and NMR[7] although a cusp at the transition temperature is observed in uniform susceptibility.[8,9] There are at least two common properties between these compounds. At first, these compounds have cubic crystal structure. Secondly, the crystalline electric field (CEF) ground states of corresponding level schemes are quartet states, which are available only in cubic systems. It is thought that the quartet state is responsible for multipole ordering.

Recently, some anomalous properties have been observed in the tetragonal metallic compound YbRu$_2$Ge$_2$.[10] In specific heat measurement without magnetic field, there are three transition temperatures at $T_0 = 10.2$ K, $T_1 = 6.5$ K, and $T_2 = 5.7$ K. It is important that the entropy around T_0 obtained by integration of specific heat data is very close to $R \ln 4$, which means the existence of a quasiquartet state even in the tetragonal system. Applying a magnetic field perpendicular to [001] direction, the specific heat jump at T_0 broadens, and the peak position corresponding to T_0 seems to increase, while T_1 and T_2 merge and decrease. Increasing magnetic field further above 7 T, no anomaly is found. On the other hand, in magnetic field parallel to [001], not only T_1 and T_2 but also T_0 decrease with increasing magnetic field. For the magnetic susceptibility χ_{ab} in magnetic field perpendicular to [001], no anomaly appears at T_0, while a cusp is observed at T_1 for small magnetic fields. Furthermore, a metamagnetic transition at higher fields around 2 T is regarded as spin-flop transition. The magnetic susceptibility χ_c in field parallel to [001] is almost temperature independent between T_0 and T_1, and shows flat temperature dependence below T_1 after a

slight decrease just below T_1. Because the value of the paramagnetic effective moment $4.5\mu_B$ is very close to magnetic moment of free Yb^{3+}, it is a reasonable assumption that *f* hole of Yb^{3+} is almost localized. Considering the quasiquartet state in a localized picture, some multipole moments will be active at each site in the system. From these experimental data, it has been suggested that T_0 is a kind of quadrupole transition, while the phase below T_1 is regarded as antiferromagnetic phase with planar staggered moment.[10] According to Jeevan *et al.*, a change in magnetic structure may happen at T_2. We will ignore this subtlety in the following and consider only T_1.

In the theoretical analysis of CeB$_6$, Shiina *et al.* have provided a mean-field approximation for the effective Hamiltonian of localized *f* electrons belonging to Γ_8-irreducible representation in O$_h$ point group. In this case, all multipole moments up to octupole are active.[11] The relevant multipoles have been classified according to irreducible representations of the point group in zero magnetic field. Taking into account that some symmetry operations of O$_h$ point group elements are lost in a magnetic field, the multipoles have been reclassified according to irreducible representations of the relevant point group in the magnetic field. Using these multipoles, a mean-field approximation has been applied to an effective Hamiltonian to construct the *H-T* phase diagram. After introduction of anisotropic interaction of quadrupoles, they have obtained a consistent explanation for the anomalous ordering in CeB$_6$. It should be noted that this approach is promising for multipole ordering not only in CeB$_6$ but also in TmTe,[12] where Tm^{2+} has the same ($4f$) (Ref. 13) electronic configuration as Yb^{3+} and NpO$_2$.[13]

In the present work, we apply this approach to investigate the phases of YbRu$_2$Ge$_2$. In this system, there are some significant differences to CeB$_6$, though a kind of quadrupole ordering is expected. At first, the crystal structure of YbRu$_2$Ge$_2$ is tetragonal, with point group D_{4h}. Second, noting that composition of the quasiquartet depends on crystalline electric field parameters, it is expected that multipole ordering is also affected by the level scheme, while only the

size of coupling constants decides on the favorable multipole ordering in cubic systems.[11] Third, considering the present system is tetragonal, some multipoles are described only by *induced moments*, whose expectation value in the CEF ground state vanishes.[14,15] Especially, the second and third points bring additional complexity to identify a multipole transition. In order to explain the behavior of YbRu$_2$Ge$_2$, we introduce an effective Hamiltonian in the next section. Then, we apply a mean-field approximation for the Hamiltonian to identify the nonmagnetic ordering state below T_0. Furthermore, we try to reproduce temperature dependences of specific heat and uniform susceptibility in magnetic field with anisotropic magnetic interaction. Finally, we summarize our results.

II. EFFECTIVE HAMILTONIAN

From analysis of uniform susceptibility, effective moment is estimated as $4.5\mu_B$, which is quite close to the value $4.54\mu_B$ for free Yb^{3+} ions. This means that the picture of localized hole in the $4f$ shell will be reasonable for YbRu$_2$Ge$_2$. First, we need to construct CEF level scheme of Yb^{3+}, to extract relevant multipole moments, and then we introduce effective intersite interactions between the multipole moments.

A. Crystalline electric field term

The total angular momentum j of Yb^{3+} ion is $j=7/2$. The multiplet splits into four Kramers doublets in tetragonal crystal structure of YbRu$_2$Ge$_2$. In tetragonal point group D_{4h}, $j=7/2$ multiplet is classified according to two-Γ_6- and two-Γ_7-irreducible representations. For two doublets belonging to the same Γ-irreducible representation, we call the lower and higher ones $\Gamma^{(1)}$ and $\Gamma^{(2)}$, respectively, in the following. These states are described by linear combination of free ion states $|\mu\rangle=|j\mu\rangle$ ($|\mu|\leq \frac{7}{2}$) as follows:

$$|\tau=1,\pm\rangle=|\Gamma_6^{(1)}\pm\rangle=\alpha_{11}\left|\frac{\pm 7}{2}\right\rangle+\alpha_{12}\left|\frac{\mp 1}{2}\right\rangle, \quad (1)$$

$$|\tau=2,\pm\rangle=|\Gamma_6^{(2)}\pm\rangle=\alpha_{21}\left|\frac{\pm 7}{2}\right\rangle+\alpha_{22}\left|\frac{\mp 1}{2}\right\rangle, \quad (2)$$

$$|\tau=3,\pm\rangle=|\Gamma_7^{(1)}\pm\rangle=\beta_{11}\left|\frac{\mp 5}{2}\right\rangle+\beta_{12}\left|\frac{\pm 3}{2}\right\rangle, \quad (3)$$

$$|\tau=4,\pm\rangle=|\Gamma_7^{(2)}\pm\rangle=\beta_{21}\left|\frac{\mp 5}{2}\right\rangle+\beta_{22}\left|\frac{\pm 3}{2}\right\rangle, \quad (4)$$

where μ is z component of total angular momentum and $+$ ($-$) of left-hand side shows pseudospin up (down) in Kramers doublets.

Usually, CEF parameters are estimated by fitting calculated uniform susceptibility to the observed one. In addition, the inelastic neutron scattering (INS) gives important informations such as splitting energy between the ground- and first-excited states in the level scheme. In recent INS experiment in YbRu$_2$Ge$_2$, the level scheme is reported with the

splitting energy of 0.9 meV.[16] Using the splitting energy, we have carried out the fitting of uniform susceptibility. Unfortunately, we could not obtain unique CEF level scheme from this procedure. However, from reasonable CEF level schemes, we obtain the following common features: (1) The splitting energy between the ground- and first-excited states is about 12 K, which is estimated by reproducing the entropy obtained from specific heat data; (2) the ground and first-excited states consist of one Γ_6 and one Γ_7 states, neither two Γ_6 nor two Γ_7 states; and (3) energy splittings of the second excited state from the ground state are at least 30 times larger than the observed transition temperature $T_0=10.2$ K and the splitting energy between the ground- and first-excited states. Due to the third point, we can neglect upper two doublets, if we consider only low temperature region. The relevant CEF Hamiltonian is then given by

$$H_{\text{CEF}}=-\sum_{\mathbf{i},\eta}\frac{\Delta_0}{2}(f_{\mathbf{i}6\eta}^\dagger f_{\mathbf{i}6\eta}-f_{\mathbf{i}7\eta}^\dagger f_{\mathbf{i}7\eta}), \quad (5)$$

where Δ_0 is splitting energy from $\Gamma_6^{(1)}$ state to $\Gamma_7^{(1)}$ state. Here, $f_{\mathbf{i}\tau\eta}^\dagger$ is creation operator of f hole with pseudospin η in $\Gamma_\tau^{(1)}$ Kramers doublet at site $\mathbf{i}$. Although we assume that the lower two doublets consist of one Γ_6 and one Γ_7 states, this assumption will be justified during identification of nonmagnetic ordered state in YbRu$_2$Ge$_2$.

B. Zeeman term

The Zeeman term due to the applied field $\mathbf{h}$ is given by

$$H_Z=-g_J\mu_B\sum_{\mathbf{i}}\mathbf{h}\cdot\mathbf{J_i}, \quad (6)$$

where $\mathbf{J}$, g_J, and μ_B are total angular momentum, Landé g factor of Yb^{3+}, and Bohr magneton, respectively. With use of second quantization, x and z components of the angular momentum in Γ_6-Γ_7 subspace are expressed as

$$J^z=c_{66}^z S_{66}^z+c_{77}^z S_{77}^z, \quad (7)$$

$$J^x=c_{66}^x S_{66}^x+c_{77}^x S_{77}^x+c_{67}^x\frac{1}{\sqrt{2}}(S_{67}^x+S_{76}^x), \quad (8)$$

with α component of pseudospin operator given by

$$S_{\tau\tau'}^\alpha=\frac{1}{2}\sum_{\eta,\eta'}f_{\tau\eta}^\dagger\sigma_{\eta\eta'}^\alpha f_{\tau'\eta'}, \quad (9)$$

where σ^α is α component of Pauli matrix. The coefficients $c_{\tau\tau'}^\alpha$ are expressed by α_{12} and β_{12} as

$$c_{66}^z=7-8\alpha_{12}^2, \quad c_{77}^z=-5+8\beta_{12}^2, \quad (10)$$

$$c_{66}^x=4\alpha_{12}^2, \quad c_{77}^x=4\sqrt{3}\beta_{12}\sqrt{1-\beta_{12}^2},$$

$$c_{67}^x=\sqrt{7}\sqrt{(1-\alpha_{12}^2)(1-\beta_{12}^2)}+\sqrt{30}\alpha_{12}\beta_{12}. \quad (11)$$

Therefore, the coefficients α_{12} and β_{12} which determine the structure of $\Gamma_6^{(1)}$ and $\Gamma_7^{(1)}$ states are incorporated through an-

isotropic effective g factors in Eqs. (7) and (8). We comment on the limiting case of $\alpha_{12}=\beta_{12}=1$, which are very close to values estimated by fitting of uniform susceptibility in Sec. III B. As we have mentioned above, we consider only quasi-quartet consisting of one Γ_6 and one Γ_7 doublet at each site. As far as the quasiquartet is concerned, multipole moments up to octupole are relevant as given in Table I. In this sense, the intersite term will be always mapped to $j=3/2$ quartet system. In particular, with $\alpha_{12}=\beta_{12}=1$, the two Kramers doublets reduce to $|\pm\frac{1}{2}\rangle$ and $|\pm\frac{3}{2}\rangle$, which belong to Γ_6- and Γ_7-irreducible representations in D_{4h} point group. In addition, the operator J^z in $j=3/2$ quartet system is the same as the operator given in Eq. (7) with $\alpha_{12}=\beta_{12}=1$. Therefore, when a magnetic field is applied in [001] direction, the present system with $\alpha_{12}=\beta_{12}=1$ is mapped to $j=3/2$ quartet system. However, such mapping is not applicable in magnetic field perpendicular along [001], due to differences of matrix elements of J^x and J^y between $j=3/2$ quartet system and the present system with $\alpha_{12}=\beta_{12}=1$.

C. Intersite term

In the present case, we consider that f hole localizes at each Yb site. From the simplification mentioned above, we have one Γ_6 doublet and one Γ_7 doublet. Even in the simplification, there are 15 kinds of multipoles at each Yb site. In order to describe the multipoles, we introduce bases of multipoles ϕ_n^Γ belonging to Γ-irreducible representation in D_{4h} point group. In Table I, we classify ϕ_n^Γ according to irreducible representations in D_{4h} point group, where in addition to $S_{\tau\tau'}^\alpha$, we use an f-charge operator

$$\rho_{\tau\tau'} = \frac{1}{2}\sum_\eta f_{\tau\eta}^\dagger f_{\tau'\eta}. \qquad (12)$$

Since classification of multipoles up to octupole is also shown in Table I, correspondence between multipole and ϕ_n^Γ will be clear. For example, the x component of dipole moment J^x is described by a linear combination of $\phi_{nx}^{\Gamma_5^-}$, which is consistent with Eq. (8).

Now, considering that metallic behavior has been observed in YbRu$_2$Ge$_2$, effective RKKY interactions between the multipoles are present, which are derived through the Schrieffer-Wolff transformation from hybridization term between $4f$ and conduction electrons. Noting that the Yb sites in the compound form body-centered tetragonal lattice, inter-layer interactions should favor ferrotype order, since antiferrocouplings would lead to frustration. In the following, we consider multipole ordering within a mean-field theory for Yb in the body-centered tetragonal structure, assuming that the ordering takes place either at the zone center $\tilde{\mathbf{q}}=0$ (ferro) or at the zone boundary $\tilde{\mathbf{q}}=(\pi,\pi,0)$ (antiferro). If we consider only diagonal term of nearest-neighbor couplings, the intersite term of Hamiltonian H_{int} is given by

$$H_{\text{int}} = -\sum_{\mathbf{i}\neq\mathbf{j}}\sum_{\Gamma,n} J_{\mathbf{i}-\mathbf{j}n}^\Gamma \phi_{\mathbf{i}n}^\Gamma \phi_{\mathbf{j}n}^\Gamma, \qquad (13)$$

TABLE I. Classification of multipoles and relevant bases of the multipoles ϕ_n^Γ according to irreducible representations of D_{4h} point group. The first column shows irreducible representation of D_{4h}. The second and third ones describe multipoles and ϕ_n^Γ belonging to Γ-irreducible representation, respectively. Here J, O, and T in the second column are dipole, quadrupole, and octupole moments, respectively. The fourth column shows expression of corresponding local susceptibility of ϕ_n^Γ with splitting energy Δ from Γ_6 to Γ_7 states. The superscript $\pm$ of irreducible representation expresses the parity with respect to time reversal.

$\Gamma\ (D_{4h})$	Multipole	ϕ_n^Γ	$\chi_{nn}^{L\Gamma}$
Γ_1^+	O_2^0	$\phi^{\Gamma_1^+}=\frac{1}{\sqrt{2}}(\rho_{66}-\rho_{77})$	$\frac{1}{8T}\left(1-\tanh^2\frac{\Delta}{2T}\right)$
Γ_3^+	O_2^2	$\phi^{\Gamma_3^+}=\frac{1}{\sqrt{2}}(\rho_{67}+\rho_{76})$	$\frac{1}{4\Delta}\tanh\frac{\Delta}{2T}$
Γ_4^+	O_{xy}	$\phi^{\Gamma_4^+}=\frac{i}{\sqrt{2}}(S_{67}^z-S_{76}^z)$	$\frac{1}{4\Delta}\tanh\frac{\Delta}{2T}$
Γ_5^+	O_{yz}	$\phi_x^{\Gamma_5^+}=\frac{i}{\sqrt{2}}(S_{67}^x-S_{76}^x)$	$\frac{1}{4\Delta}\tanh\frac{\Delta}{2T}$
	O_{zx}	$\phi_y^{\Gamma_5^+}=\frac{i}{\sqrt{2}}(S_{67}^y-S_{76}^y)$	$\frac{1}{4\Delta}\tanh\frac{\Delta}{2T}$
Γ_2^-	J^z	$\phi_1^{\Gamma_2^-}=S_{66}^z$	$\frac{1}{8T}\left(1+\tanh\frac{\Delta}{2T}\right)$
	T_z^α	$\phi_2^{\Gamma_2^-}=S_{77}^z$	$\frac{1}{8T}\left(1-\tanh\frac{\Delta}{2T}\right)$
Γ_3^-	T_{xyz}	$\phi^{\Gamma_3^-}=\frac{i}{\sqrt{2}}(\rho_{67}-\rho_{76})$	$\frac{1}{4\Delta}\tanh\frac{\Delta}{2T}$
Γ_4^-	T_z^β	$\phi^{\Gamma_4^-}=\frac{1}{\sqrt{2}}(S_{67}^z+S_{76}^z)$	$\frac{1}{4\Delta}\tanh\frac{\Delta}{2T}$
Γ_5^-	J^x	$\phi_{1x}^{\Gamma_5^-}=S_{66}^x$	$\frac{1}{8T}\left(1+\tanh\frac{\Delta}{2T}\right)$
	T_x^α	$\phi_{2x}^{\Gamma_5^-}=S_{77}^x$	$\frac{1}{8T}\left(1-\tanh\frac{\Delta}{2T}\right)$
	T_x^β	$\phi_{3x}^{\Gamma_5^-}=\frac{1}{\sqrt{2}}(S_{67}^x+S_{76}^x)$	$\frac{1}{4\Delta}\tanh\frac{\Delta}{2T}$
	J^y	$\phi_{1y}^{\Gamma_5^-}=S_{66}^y$	$\frac{1}{8T}\left(1+\tanh\frac{\Delta}{2T}\right)$
	T_y^α	$\phi_{2y}^{\Gamma_5^-}=S_{77}^y$	$\frac{1}{8T}\left(1-\tanh\frac{\Delta}{2T}\right)$
	T_y^β	$\phi_{3y}^{\Gamma_5^-}=\frac{1}{\sqrt{2}}(S_{67}^y+S_{76}^y)$	$\frac{1}{4\Delta}\tanh\frac{\Delta}{2T}$

$$= -\frac{1}{N_0}\sum_{\Gamma,n}\sum_{\mathbf{q}} J_n^\Gamma(\mathbf{q})\phi_n^\Gamma(-q)\phi_n^\Gamma(\mathbf{q}), \qquad (14)$$

with $\phi_n^\Gamma(\mathbf{q})=\Sigma_{\mathbf{i}}e^{-i\mathbf{q}\cdot\mathbf{i}}\phi_{\mathbf{i}n}^\Gamma$, where J_n^Γ is a coupling constant between ϕ_n^Γ, and N_0 is the number of Yb sites in crystal. In Eq.

(14), $J_n^\Gamma(\mathbf{q})$ and $\phi_n^\Gamma(\mathbf{q})$ are Fourier components of coupling constants and $\phi_{\mathbf{i}n}^\Gamma$, respectively. For square lattice, $J_n^\Gamma(\mathbf{q})$ is given by

$$J_n^\Gamma(\mathbf{q}) = 2J_n^\Gamma(\cos q_x + \cos q_y). \qquad (15)$$

D. Resulting effective Hamiltonian

In order to explain low temperature property of YbRu$_2$Ge$_2$, effective Hamiltonian used in the following is described by

$$H_{\text{eff}} = H_{\text{CEF}} + H_Z + H_{\text{int}}. \qquad (16)$$

As we have already mentioned, we can determine $|\Delta_0|$ from the entropy. However, in Zeeman term H_Z, there are two free parameters, which control the weights of $|\pm 1/2\rangle$ and $|\pm 3/2\rangle$ in $\Gamma_6^{(1)}$ and $\Gamma_7^{(1)}$ states, respectively. In addition, we have coupling constants J_n^Γ, which will be estimated in the following sections. Then we apply a mean-field approximation for the effective Hamiltonian to calculate thermodynamic quantities and the phase diagrams.

III. ANALYSIS OF TRANSITION AT T_0

In this section, we develop a mean-field theory for the effective Hamiltonian to analyze nonmagnetic transition at T_0. After comparing phase diagrams for all types of ferro- and antiferroquadrupole orderings with experimental one, we propose a preferred type of quadrupole order in YbRu$_2$Ge$_2$.

A. Mean-field approximation for quadrupolar order

At first, we give mean-field Hamiltonian to determine transition line in H-T phase diagram. We assume that multipole ordered state is specified by irreducible representation Γ and ordering wave vector $\tilde{\mathbf{q}}$. From the effective model, we obtain easily the mean-field Hamiltonian

$$H_{\text{MF}} = H_{\text{CEF}} + H_Z + \tilde{H}_{\text{int}}, \qquad (17)$$

$$\tilde{H}_{\text{int}} = -\frac{1}{N_0} \sum_{\Gamma,n} \sum_{\mathbf{q}} J_n^\Gamma(\mathbf{q})(2\langle\phi_n^\Gamma(\mathbf{q})\rangle\phi_n^\Gamma(\mathbf{q}) - \langle\phi_n^\Gamma(\mathbf{q})\rangle^2),$$
$$(18)$$

with

$$\langle\cdots\rangle = \frac{\text{Tr } e^{-H_{\text{MF}}/T}\cdots}{\text{Tr } e^{-H_{\text{MF}}/T}}, \qquad (19)$$

where T is the temperature.

We consider three cases, (1) system in zero magnetic field, (2) system in magnetic field parallel to [001] direction, and (3) system in magnetic field parallel to [100] direction, whose point groups are D_{4h}, C_{4v}, and C_{2v}, respectively. In Tables II and III, bases of multipoles are classified according to irreducible representations of C_{4v} and C_{2v} point groups, respectively. In order to develop a general formalism, we call bases of multipoles belonging to Γ-irreducible representation generically ψ_n^Γ in any point group G (D_{4h}, C_{4v}, and C_{2v}). For

TABLE II. Classification of ϕ_n^Γ according to irreducible representations of C_{4v}, which is point group of tetragonal system in magnetic field parallel to [001]. Here, we note that ϕ_n^Γ are bases of multipoles belonging to Γ-irreducible representation in D_{4h} point group. The first column shows irreducible representation of C_{4v}. The second, third, and fourth ones describe quadrupoles, $\phi_n^{\Gamma^+}$, and $\phi_n^{\Gamma^-}$ belonging to each irreducible representation in C_{4v}, respectively.

Γ (C_{4v})	O	$\phi_n^{\Gamma^+}$ (Even)	$\phi_n^{\Gamma^-}$ (odd)
Γ_1	O_2^0	$\phi^{\Gamma_1^+} = \frac{1}{\sqrt{2}}(\rho_{66}-\rho_{77})$	$\phi_1^{\Gamma_2^-} = S_{66}^z$
			$\phi_2^{\Gamma_2^-} = S_{77}^z$
Γ_3	O_2^2	$\phi^{\Gamma_3^+} = \frac{1}{\sqrt{2}}(\rho_{67}+\rho_{76})$	$\phi^{\Gamma_4^-} = \frac{1}{\sqrt{2}}(S_{67}^z+S_{76}^z)$
Γ_4	O_{xy}	$\phi^{\Gamma_4^+} = \frac{i}{\sqrt{2}}(S_{67}^z-S_{76}^z)$	$\phi^{\Gamma_3^-} = \frac{i}{\sqrt{2}}(\rho_{67}-\rho_{76})$
Γ_5	O_{yz}	$\phi_x^{\Gamma_5^+} = \frac{i}{\sqrt{2}}(S_{67}^x-S_{76}^x)$	$\phi_{1y}^{\Gamma_5^-} = S_{66}^y$
			$\phi_{2y}^{\Gamma_5^-} = S_{77}^y$
			$\phi_{3y}^{\Gamma_5^-} = \frac{1}{\sqrt{2}}(S_{67}^y+S_{76}^y)$
	O_{zx}	$\phi_y^{\Gamma_5^+} = \frac{i}{\sqrt{2}}(S_{67}^y-S_{76}^y)$	$\phi_{1x}^{\Gamma_5^-} = S_{66}^x$
			$\phi_{2x}^{\Gamma_5^-} = S_{77}^x$
			$\phi_{3x}^{\Gamma_5^-} = \frac{1}{\sqrt{2}}(S_{67}^x+S_{76}^x)$

D_{4h} point group, ψ_n^Γ is equivalent to ϕ_n^Γ given in Table. I. For nonzero field, the corresponding lower symmetry point groups C_{4v} and C_{2v} have basis functions ψ_n^Γ that may still be directly expressed in terms of the D_{4h} basis functions ϕ_n^Γ, as shown in Tables II and III. In the following, we discuss only disordered, ferro-, and antiferro-ordered states, which is reasonable since we restrict to nearest-neighbor interaction in H_{int}. In the disordered state, only the fully symmetric multipole $\psi_n^{\Gamma_1}$ (O_2^0 in zero field) has a nonzero expectation value $\langle\psi_n^{\Gamma_1}(\mathbf{0})\rangle$. It leads to the background temperature dependence of Γ_6-Γ_7 splitting, as shown later. In ferro-ordered state belonging to Γ-irreducible representation, $\langle\psi_n^\Gamma(\mathbf{0})\rangle$ have finite values in addition to $\langle\psi_n^{\Gamma_1}(\mathbf{0})\rangle$. In antiferro-ordered state belonging to Γ-irreducible representation, allowed expectation values are $\langle\psi_n^\Gamma(\tilde{\mathbf{q}})\rangle$ and $\langle\psi_n^{\Gamma_1}(\mathbf{0})\rangle$.

For transition from disordered state to either ferro-or antiferromultipole ordered state, we usually consider first- and second-order transitions. In a ferro (or antiferro) multipole ordered state belonging to Γ-irreducible representation in point group, expectation values of multipole moments $\langle\psi_n^\Gamma(\mathbf{0})\rangle$ (or $\langle\psi_n^\Gamma(\tilde{\mathbf{q}})\rangle$) have nonzero values. In general, free energy of ordered state is lower than that of disordered state

TABLE III. Classification of ϕ_n^Γ according to irreducible representations of C_{2v}, which is point group of tetragonal system in magnetic field parallel to [100]. Here, we note that ϕ_n^Γ are bases of multipoles belonging to Γ irreducible representation in D_{4h} point group. The first column shows irreducible representation of C_{2v}. The second, third, and fourth ones describe quadrupoles, $\phi_n^{\Gamma^+}$, and $\phi_n^{\Gamma^-}$ belonging to each irreducible representation in C_{2v}, respectively.

Γ (C_{2v})	O	$\phi_n^{\Gamma^+}$ (Even)	$\phi_n^{\Gamma^-}$ (Odd)
Γ_1	O_2^0	$\phi^{\Gamma_1^+}=\dfrac{1}{\sqrt{2}}(\rho_{66}-\rho_{77})$	$\phi_{1x}^{\Gamma_5^-}=S_{66}^x$
	O_2^2	$\phi^{\Gamma_3^+}=\dfrac{1}{\sqrt{2}}(\rho_{67}+\rho_{76})$	$\phi_{2x}^{\Gamma_5^-}=S_{77}^x$
			$\phi_{3x}^{\Gamma_5^-}=\dfrac{1}{\sqrt{2}}(S_{67}^x+S_{76}^x)$
Γ_2	O_{yz}	$\phi_x^{\Gamma_5^+}=\dfrac{i}{\sqrt{2}}(S_{67}^x-S_{76}^x)$	$\phi^{\Gamma_3^-}=\dfrac{i}{\sqrt{2}}(\rho_{67}-\rho_{76})$
Γ_3	O_{xy}	$\phi^{\Gamma_4^+}=\dfrac{i}{\sqrt{2}}(S_{67}^z-S_{76}^z)$	$\phi_{1y}^{\Gamma_5^-}=S_{66}^y$
			$\phi_{2y}^{\Gamma_5^-}=S_{77}^y$
			$\phi_{3y}^{\Gamma_5^-}=\dfrac{1}{\sqrt{2}}(S_{67}^y+S_{76}^y)$
Γ_4	O_{zx}	$\phi_y^{\Gamma_5^+}=\dfrac{i}{\sqrt{2}}(S_{67}^y-S_{76}^y)$	$\phi_1^{\Gamma_2^-}=S_{66}^z$
			$\phi_2^{\Gamma_2^-}=S_{77}^z$
			$\phi^{\Gamma_4^-}=\dfrac{1}{\sqrt{2}}(S_{67}^z+S_{76}^z)$

below the transition temperature. The explicit expression of free energy in mean-field approximation has already been given by Shiina *et al.*[11] In particular, if the transition is of second order, all order parameters continuously reduce to zero on approaching the transition point. We use linearized mean-field equation to determine the second-order transition point, by expanding the partition function with respect to $\tilde{H}_{\text{int}}$ given in Eq. (18). For transition to ordered state specified by irreducible representation Γ of point group and ordering wave vector $\tilde{\mathbf{q}}$, it is given by

$$\langle\psi_n^\Gamma(\tilde{\mathbf{q}})\rangle = \sum_m \chi_{nm}^{L\Gamma} 2J_m^\Gamma(\tilde{\mathbf{q}})\langle\psi_m^\Gamma(\tilde{\mathbf{q}})\rangle, \qquad (20)$$

with local susceptibility $\chi_{nn'}^{L\Gamma}$ defined by

$$\chi_{nn'}^{L\Gamma} = \int_0^{1/T} d\tau\langle\psi_{\text{in}}^\Gamma(\tau)\psi_{\text{in}'}^\Gamma\rangle - \delta_{\Gamma=\Gamma_1}\frac{\langle\psi_{\text{in}}^{\Gamma_1}\rangle\langle\psi_{\text{in}'}^{\Gamma_1}\rangle}{T}, \qquad (21)$$

where τ is the imaginary time coordinate. The $\chi_{nn'}^{L\Gamma}$ are calculated in the limit of $\langle\psi_n^\Gamma(\tilde{\mathbf{q}})\rangle\to 0$. The linearized mean-field

equation has nontrivial solution only when the maximum eigenvalue of $2\hat{\chi}^{L\Gamma}J_m^\Gamma(\tilde{\mathbf{q}})$ becomes unity. We note that the transition becomes second order, only if the transition point determined by linearized mean-field equation (20) is the same point where the free energies of the two states are equal.

B. Estimation of coupling constants

In our mean-field Hamiltonian, there are various parameters Δ_0, α_{12}, β_{12}, and J_n^Γ. At first, we consider disordered state in zero magnetic field. In this case, only allowed multipole is the uniform component of $\langle\phi^{\Gamma_1^+}\rangle$. Then, Δ_0 is renormalized as

$$\Delta = \Delta_0 + \frac{1}{2}J^{\Gamma_1^+}(0)\tanh\frac{\Delta}{2T}. \qquad (22)$$

For estimation of Δ_0 and $J^{\Gamma_1^+}(0)=4J^{\Gamma_1^+}$, we assume $\Delta(T=12\text{ K})=12$ K and $\Delta_0=8$ K, which gives $\Delta(T=T_0=10.2\text{ K})=12.8$ K and $J^{\Gamma_1^+}=4.3$ K. By choosing these parameter values, we obtain reasonable temperature dependence of entropy around T_0. In the following calculation, we fix these values of Δ_0 and $J^{\Gamma_1^+}$.

Now we determine the values of α_{12} and β_{12}. These affect the magnetic anisotropy of the uniform susceptibility. Experimentally, the uniform susceptibility in magnetic field perpendicular to [001] is quite large compared to that in magnetic field parallel to [001]. The magnetic anisotropy is successfully reproduced by using the following lower two CEF states: The ground CEF state has almost pure $|\mp 1/2\rangle$ character belonging to Γ_6-irreducible representation, while the first-excited CEF state is almost pure $|\pm 3/2\rangle$ belonging to Γ_7-irreducible representation. Then the lower two CEF states are described by $\alpha_{12}\approx 1$ and $\beta_{12}\approx 1$, while $\alpha_{11}\approx\alpha_{22}\approx 0$.[16] With these values of α_{12} and β_{12}, contribution to J^z from the first-excited Γ_7 state cancels out contribution from the ground Γ_6 state, while magnitude of g-factor c_{66}^x coming from the ground Γ_6 state in magnetic field parallel to [100] is four times larger than c_{66}^z. Therefore, this CEF level scheme seems to be consistent with the observed magnetic anisotropy of the uniform susceptibility. In the following, we study transitions in the compound with these parameter values.

Furthermore, we have many interaction parameters in the intersite term. Because the highest transition takes place at T_0, each multipole interaction has an upper limit. We estimate the upper limit of each coupling constant, by assuming that the transition to each ordered state takes place at T_0 in zero field. Since we use the linearized mean-field equation (20), we need to evaluate $\chi_{nn'}^{L\Gamma}$. In D_{4h} point group, the matrix $\hat{\chi}^{L\Gamma}$ has diagonal form for each Γ. Each eigenvalue of nth component in Γ is given by

$$\lambda_n^\Gamma = 2J_n^\Gamma(\tilde{\mathbf{q}})\chi_{nn}^{L\Gamma}, \qquad (23)$$

where expressions for $\chi_{nn}^{L\Gamma}$ are summarized in fourth column in Table. I. Specifically, for each of the three two-dimensional representations, (J^x, J^y), (T_x^α, T_y^α), and (T_x^β, T_y^β) in

TABLE IV. Coupling constants used for analysis of YbRu$_2$Ge$_2$. The first column shows irreducible representation of D_{4h}. The second column shows upper limits of magnitudes of coupling constants for having ϕ_n^Γ order parameter at T_0. The third column shows coupling constants used in the model calculation of Sec. V. Here sign for J^Γ denotes ferro/antiferro coupling. The value in parentheses exhibits reduced coupling constant between $\phi_{3\bar{y}}^{\Gamma_5^-}$.

Γ (D_{4h})	$1/8 \max \chi_{nn}^{L\Gamma}$ ($T=T_0$) (K)	J^Γ [K]
Γ_1^+	14.8	4.3
Γ_3^+	11.5	11.5
Γ_4^+	11.5	-3.0
Γ_5^+	11.5	-3.0
Γ_2^-	6.6	1.7
Γ_3^-	11.5	-3.0
Γ_4^-	11.5	-3.0
Γ_5^-	6.6	-3.4 (-2.1)

Table I, we assume that the upper limit of coupling constant is independent of n. Together with one-dimensional representation, the upper limit of coupling constant for Γ-irreducible representation $J_c^\Gamma(\tilde{\mathbf{q}})$ is then given by

$$2J_c^\Gamma(\tilde{\mathbf{q}}) = \frac{1}{\max \chi_{nn}^{L\Gamma}(T=T_0)}. \tag{24}$$

In Table IV, by using the splitting energy Δ determined above, we list the calculated values of $1/8 \max \chi_{nn}^{L\Gamma}(T=T_0)$, which is equal to upper limit value of J^Γ with factor $1/2z = 1/8$, where z is the square lattice coordination number. If we use corresponding upper limit for every coupling constant, all transition temperatures to ordered states would become degenerate at T_0. In calculating the transition to an ordered state with a primary order parameter ϕ_n^Γ, we assume that only the coupling constant for ϕ_n^Γ is at the upper limit. All others are reduced by a factor $\alpha_{\Gamma'}$ ($\Gamma' \neq \Gamma$)

$$J_n^\Gamma(\tilde{\mathbf{q}}) = J_c^\Gamma(\tilde{\mathbf{q}}),$$

$$J_n^{\Gamma'}(\tilde{\mathbf{q}}) = \alpha_{\Gamma'} J_c^{\Gamma'}(\tilde{\mathbf{q}}) \quad \text{for } \Gamma' \neq \Gamma, \tag{25}$$

where $0 < \alpha_{\Gamma'} < 1$ is a ratio of actual coupling constant J^Γ to the critical value J_c^Γ. Present available experimental data do not allow a unique determination of coupling constants. Only that for the primary ferroquadrupolar order parameter may be fixed by the transition temperature T_0. In order to obtain a low-field behavior of $T_0(h)$ which is insensitive to the details of the model we assume $\alpha_{\Gamma'} = 0.5$ for the remaining coupling strengths.

C. Order parameter candidates for transition at T_0

Before we discuss candidates for transition at T_0, we note a property of lower two CEF states for magnetic field parallel to [001]. As we have mentioned in previous subsection, the ground CEF state belonging to Γ_6 is lower than the first-excited CEF state belonging to Γ_7 by 12.8 K at T_0 in zero
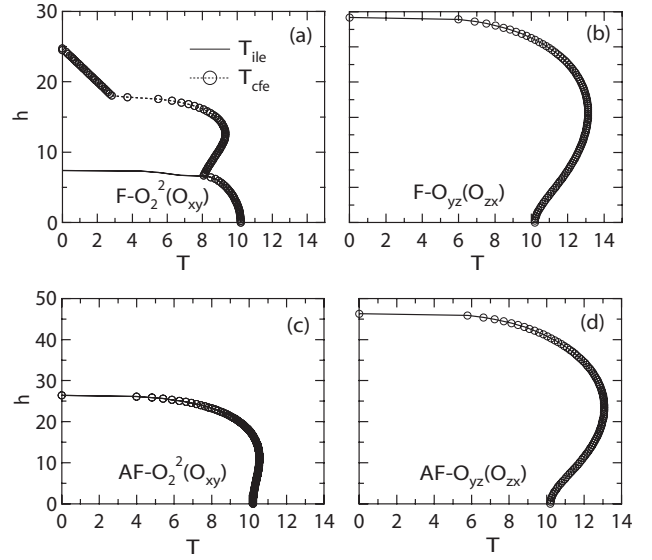
FIG. 1. h-T phase diagrams for quadrupole ordered states. The solid line determined by linearized mean-field equation. The open circle is given by comparison of free energies between disordered state and corresponding quadrupole ordering state. When these instability points are (not) the same, the transition is of second order (first order). It should be noted that $h_c'(T_0) = \infty$ in (a)–(d), which has been shown in Appendix B of Ref. 11.

magnetic field. Since the magnetic field parallel to [001] does not break fourfold symmetry, we still can distinguish the Γ_6 and Γ_7 states. In this case their energies are easily obtained as $-\frac{\Delta}{2} \mp g_J \mu_B c_{66}^z h$ for the Γ_6 Kramers doublet and $\frac{\Delta}{2} \mp g_J \mu_B c_{77}^z h$ for the Γ_7 state. There are two remarkable points in the present level scheme; (1) c_{66}^z has negative sign while c_{77}^z is positive, and (2) magnitude of c_{77}^z is three times larger than that of c_{66}^z. From these facts, we can expect a level crossing in the high-field region of the disordered phase, where the CEF ground state changes from Γ_6 in low field to Γ_7 in high field.[17]

In the following, we discuss the transition line of $T_0(h)$ in magnetic field parallel to [001]. From experimental result, the specific heat data show that the transition temperature of the nonmagnetic phase decreases with increasing magnetic field. As mentioned before, we assume that the nonmagnetic transition is obtained by ordering of quadrupole moment. However, we do not know the character of the quadrupole moment among the possible O_2^0, O_2^2, O_{xy}, and (O_{yz}, O_{zx}) cases, and even whether the ordering is of ferro-or antiferro-type. In order to identify the type of quadrupole ordering, we calculate transition lines for all kinds of quadrupole orderings to compare with the experimental one. First, since coupling constant between O_2^0 is ferrolike as estimated in the previous subsection, and ferrocomponent of O_2^0 is allowed even in the disordered state belonging to Γ_1 in C_{4v} point group (Table II), we exclude any ordering of O_2^0 from candidates of the transition at T_0. It does not break any symmetry and hence cannot lead to a specific heat jump. Second, we show transition lines for other types of quadrupole orderings in Fig. 1, where for coupling constants other than the primary order parameter, $\alpha_{\Gamma'} = 0.5$ is chosen. Considering the
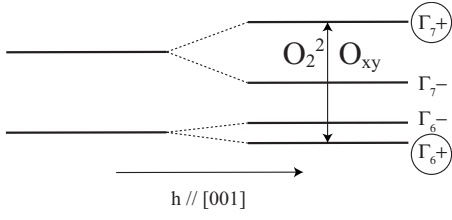
FIG. 2. Schematic view of lower two CEF states in magnetic field parallel to [001]. By operators of O_2^2 and O_{xy}, which are equivalent to $\phi^{\Gamma_3^+} = \frac{1}{\sqrt{2}}(\rho_{67} + \rho_{76})$ and $\phi^{\Gamma_4^+} = \frac{i}{\sqrt{2}}(S_{67}^z - S_{76}^z)$, respectively, the ground Γ_6 state couples only with the highest Γ_7 state in low magnetic field region. This leads to the induced type quadrupole order below T_0. The energy difference between these two states increases with increasing magnetic field.

behavior of experimental specific heat, ferro-O_2^2 and ferro-O_{xy} orderings are consistent with the experiment among all types of quadrupole orderings. From calculated results, we conclude that transition to ferro-O_2^2 (or ferro-O_{xy}) ordering state is of second order in low magnetic field region. In order to explain a decrease of transition temperature in the magnetic field, we show schematic view of magnetic field dependence of level scheme with possible transitions for O_2^2 and O_{xy} in Fig. 2. In both O_2^2 and O_{xy} ordering states, the ground CEF state $|\Gamma_6+\rangle$ couples only with highest state $|\Gamma_7+\rangle$; therefore, O_2^2 and O_{xy} orders are of induced type because the quadrupole expectation value in the ground state vanishes. In addition, splitting energy between these states increases with increasing magnetic field. Then, since the energy denominator of the dominant term of corresponding local susceptibility, Eq. (21), increases, the second-order transition temperature decreases with increasing magnetic field. On the other hand, for ordering of O_{yz} or O_{zx}, transition temperature of these quadrupole orderings increases with increasing magnetic field, since splitting energy between the ground CEF state and excited state $|\Gamma_7-\rangle$ decreases.

We now consider behavior in magnetic field perpendicular to [001]. From specific heat experiment, it is shown that the anomaly of specific heat jump broadens with increasing magnetic field. This means that the transition at T_0 in zero magnetic field reduces to a crossover in magnetic field perpendicular to [001]. We note that crossover does not break any symmetry. Instead of transition temperature T_0, we define a characteristic temperature T^* as an inflection point of the specific heat divided by temperature. Let us assume antiferroquadrupole ordering, which breaks at least translational symmetry. Since this would cause a specific heat jump, we exclude antiferroquadrupole ordered state from the scenario of crossover. On the other hand, ferroquadrupole ordering in general breaks local rotational symmetry, although the translational symmetry is preserved. However, ferroquadrupole ordering belonging to Γ_1-irreducible representation neither breaks translational symmetry nor rotational symmetry. For the system in magnetic field parallel to [100], O_2^0 and O_2^2 belong to Γ_1-irreducible representation, given in Table III. We note again that ferro-O_2^0 ordering does not break any symmetry for any field direction and therefore is excluded. Thus, we have one scenario that T^* will be a crossover temperature from usual high temperature region to low temperature region where a considerable ferro-O_2^2 component appears.

We now consider magnetic field along the [110] direction, which is also perpendicular to tetragonal c axis. If we repeat similar discussion as for the [100] direction, the only possible ordering is ferro-O_{xy} belonging to Γ_1-irreducible representation in corresponding point group (see Table V), instead of ferro-O_2^2. Unfortunately, we cannot distinguish ferro-O_2^2 from ferro-O_{xy} ordering, because the anisotropy in ab plane is not clarified below T_0 from the present experimental data. Therefore, in order to distinguish the type of quadrupole ordering in YbRu$_2$Ge$_2$, determination of different thermodynamical properties for two magnetic field directions, [001] and [110], is required. In particular, the possible lattice distortion induced by the quadrupole ordering should be investigated. Furthermore, determination of elastic constant softening would be desirable.

In addition, we consider difference of nonmagnetic multipole moments between two Γ_6 (two Γ_7) level scheme and the Γ_6-Γ_7 system. In the case of Γ_6-Γ_7 level scheme, nonmagnetic multipole moments are summarized in Tables I–III and V, where O_2^2 and O_{xy} are described by linear combination of off-diagonal operators $\rho_{\tau\tau'}$ and $S_{\tau\tau'}^z$ with orbital indices $\tau \neq \tau'$, respectively. On the other hand, in the cases of two Γ_6 and two Γ_7 level schemes, corresponding orbital off-diagonal operators are not of quadrupole type and belong to Γ_1 and Γ_2-irreducible representations in D_{4h} and C_{4v} point

TABLE V. Classification of ϕ_n^Γ according to irreducible representations of C_{2v}, which is point group of tetragonal system in magnetic field parallel to [110]. Here, we note that ϕ_n^Γ are bases of multipoles belonging to Γ-irreducible representation in D_{4h} point group. The first column shows irreducible representation of C_{2v}. The second, third, and fourth ones describe quadrupoles, $\phi_n^{\Gamma^+}$, and $\phi_n^{\Gamma^-}$ belonging to each irreducible representation in C_{2v}, respectively.

Γ (C_{2v})	Quadrupole	$\phi_n^{\Gamma^+}$ (Even)	$\phi_n^{\Gamma^-}$ (Odd)
Γ_1	O_2^0	$\phi^{\Gamma_1^+}$	$\phi_{1x}^{\Gamma_5^-} + \phi_{1y}^{\Gamma_5^-}$
	O_{xy}	$\phi^{\Gamma_4^+}$	$\phi_{2x}^{\Gamma_5^-} + \phi_{2y}^{\Gamma_5^-}$
			$\phi_{3x}^{\Gamma_5^-} - \phi_{3y}^{\Gamma_5^-}$
Γ_2	$O_{yz} - O_{zx}$	$\phi_x^{\Gamma_5^+} - \phi_y^{\Gamma_5^+}$	$\phi^{\Gamma_4^-}$
Γ_3	$O_{yz} + O_{zx}$	$\phi_x^{\Gamma_5^+} + \phi_y^{\Gamma_5^+}$	$\phi_1^{\Gamma_2^-}$
			$\phi_2^{\Gamma_2^-}$
			$\phi^{\Gamma_3^-}$
Γ_4	O_2^2	$\phi^{\Gamma_3^+}$	$\phi_{1x}^{\Gamma_5^-} - \phi_{1y}^{\Gamma_5^-}$
			$\phi_{2x}^{\Gamma_5^-} - \phi_{2y}^{\Gamma_5^-}$
			$\phi_{3x}^{\Gamma_5^-} + \phi_{3y}^{\Gamma_5^-}$

groups, respectively. This is because associated Kramers doublets belong to the same irreducible representation in such level schemes. Furthermore, in C_{2v} point group these operators belong to Γ_1- and Γ_3-irreducible representations, respectively. Due to these differences of irreducible representations from those in the Γ_6-Γ_7 level scheme, no consistent explanation for transition at T_0 is obtained for level schemes with two Γ_6 or two Γ_7 doublets. Considering these arguments, only Γ_6-Γ_7 level scheme provides a reasonable explanation for the transition at T_0.

Finally, we summarize this section by proposing candidates for quadrupolar state below T_0. In this subsection, we have calculated transition lines of quadrupole ordering in magnetic field parallel to [001], and discussed specific heat jump in magnetic field perpendicular to [001]. Due to these results obtained from different point of views, only two appropriate candidates remain. The reasonable candidates for nonmagnetic transition at T_0 are ferro-O_2^2 and ferro-O_{xy} order parameters. In addition, these orders are of induced type in the magnetic field parallel to [001]. Furthermore, we stress that both ferro-O_2^2 and ferro-O_{xy} orderings can appear only for the Γ_6-Γ_7 level scheme.

IV. DISCUSSION OF THE SECOND TRANSITION AT T_1

In the previous section, we have analyzed nonmagnetic transition at T_0, and proposed either ferro-O_2^2 or ferro-O_{xy} ordering in system with Γ_6-Γ_7 level scheme. In this section, we provide some proposals for the second transition at T_1, which is below T_0. At first, we summarize experimental results below T_1. Specific heat data show[10] that a second-order phase transition appears at T_1. The transition temperature decreases with increasing magnetic field both parallel and perpendicular to [001]. Below T_1, uniform susceptibility data exhibit a clear difference between the temperature dependence of χ_c and χ_{ab}, which are the uniform susceptibilities in magnetic field parallel and perpendicular to [001], respectively. Here, χ_c seems to be independent of temperature except for a slight decrease just below T_1, while χ_{ab} shows a clear cusp at T_1 in weak magnetic field. From the difference of temperature dependence of χ_c and χ_{ab}, it has been proposed that below T_1 an antiferromagnetic state appears with staggered magnetic moment perpendicular to [001]. In addition, magnetization for field perpendicular to [001] has shown a metamagnetic transition. This has been regarded as a spin-flop transition in the ab plane.

From a theoretical point of view, time reversal symmetry must be broken eventually below nonmagnetic transition temperature T_0, in order to release remaining entropy $R \ln 2$ of the Kramers doublet ground state. In this sense, the antiferromagnetic ordering is reasonable. However, in addition to dipole (magnetic) moments, the present model has octupole moments which also break time reversal symmetry. Below the quadrupolar transition temperature T_0, the point group reduces from D_{4h} to D_{2h} in zero magnetic field, because both ferro-O_2^2 and ferro-O_{xy} orderings break only fourfold rotational symmetry. For dipole and octupole moments, there are four one-dimensional irreducible representations in D_{2h} point group. Among these four irreducible representa-

tions, three have respective components of dipole moment J^α in addition to two components of octupoles. On the other hand, the remaining irreducible representation has only one octupole component. Let us consider the uniform magnetic susceptibility in pure octupole ordered state. In very weak magnetic field, it is expected that the uniform susceptibility does not considerably decrease below the transition temperature of the octupole ordering, because there is no dipole order parameter in the state. Since this behavior is inconsistent with experimental data of χ_{ab}, we exclude the pure octupole from candidates for the ordered state below T_1. Therefore, even though we include octupole degrees of freedom, the state below T_1 seems to be inconsistent with pure octupole ordering, but rather must be an antiferromagnetic state with a considerable magnitude of the dipole moment.

As candidate below T_1, an antiferromagnetic state will be reasonable from the above discussion of the susceptibility. However, the direction of the staggered moments in the ab plane is still unclear. The direction depends on whether the ordering quadrupole moment below T_0 is O_2^2 or O_{xy} because their remaining symmetry axis is different. Let us consider ferro-O_2^2 order in magnetic field parallel to [100]. According to Table III, the allowed directions of magnetic moments in the system are $J^x\mathbf{e}_x$, $J^y\mathbf{e}_y$, and $J^z\mathbf{e}_z$, where $\mathbf{e}_x$, $\mathbf{e}_y$, and $\mathbf{e}_z$ are unit vectors parallel to [100], [010], and [001] directions, respectively. Furthermore, the direction of staggered moments in the antiferromagnetic state is perpendicular to [001] axis according to the experimental uniform susceptibility. Therefore, for magnetic transition within the O_2^2 phase, the dipole order parameter should be described by $J^x\mathbf{e}_x$ or $J^y\mathbf{e}_y$. Likewise, within the O_{xy} phase in magnetic field parallel to [110], it should be $J^x\mathbf{e}_x \pm J^y\mathbf{e}_y$. This means that determination of staggered moment direction can distinguish between quadrupole order of ferro-O_2^2 or ferro-O_{xy} type.

Now, we consider the metamagnetic transition, which has been observed in magnetic field perpendicular to [001], starting from an antiferromagnetic state with planar staggered moment. In the present scenario, the antiferromagnetism is regarded to appear below ferro-O_2^2 or ferro-O_{xy} ordering temperature. In these cases, the point group reduces from D_{4h} to D_{2h} in zero magnetic field. Consequently, two-dimensional irreducible representation in D_{4h}, which involves two planar components of magnetic moment, reduce to the direct sum of two one-dimensional irreducible representations, where each has one planar component of magnetic moment.

Then it is expected that exchange coupling constants between planar components of magnetic moments depend on the in-plane direction. These effective coupling constants are due to RKKY mechanism; therefore, their anisotropy will be induced by reconstruction of conduction electron states in the ferroquadrupolar ordered phase. This exchange anisotropy induced by quadrupole order is the origin of the spin-flop transition for $H \perp [001]$.

V. MEAN-FIELD ANALYSIS OF BOTH ORDERED PHASES

From previous discussions, we have two candidates for successive transitions; one scenario is given by ferro-O_2^2 ordering for the first transition at T_0 before the second transi-

tion at T_1 to antiferromagnetism with staggered moment $J^x\mathbf{e}_x$ or $J^y\mathbf{e}_y$, and another is ferro-O_{xy} ordering for transition at T_0 before transition at T_1 to antiferromagnetism with staggered moment $J^x\mathbf{e}_x \pm J^y\mathbf{e}_y$. In the following, we assume ferro-O_2^2 ordering for the transition at T_0, because we cannot distinguish these two possibilities from available experimental data.

A. Reestimation of coupling constants

In the previous section, we have estimated parameter values of model Hamiltonian, such that magnetic anisotropy of uniform susceptibility and nonmagnetic transition temperature are reasonably reproduced. However, in that stage, we have assumed that all signs of coupling constants are the same. In the present case, we are considering that the system shows ferroquadrupole ordering before antiferromagnetic transition. Therefore, we should estimate coupling constants with assumption of ferroquadrupole transition at T_0 and antiferromagnetic transition at T_1. Among these coupling constants, $J^{\Gamma_1^+}$ and $J^{\Gamma_3^+}$ are not changed from values used for Fig. 1(a). On the other hand, we choose value of $J^{\Gamma_5^-}$ as antiferromagnetic transition appears at $T_1 = 6.5$ K in zero magnetic field. In addition, magnitudes of other coupling constants are chosen to be small with $\alpha^{\Gamma'} = 0.25$ ($\Gamma' = \Gamma_4^+, \Gamma_5^+, \Gamma_2^-, \Gamma_3^-$, and Γ_4^-), so that unobserved phases are suppressed which would appear if $\alpha^{\Gamma'}$ were larger. Furthermore, considering that coupling constant between x components of magnetic moment is different from correspondence between y components of magnetic moment in ferro-O_2^2 ordering state, we will reduce magnitude of coupling constant between $\phi_{3y}^{\Gamma_5^-}$. In Table IV, we summarize the revised values of coupling constants.

B. Phase diagram

At first, we construct H-T phase diagram in magnetic field parallel to [001]. As we have mentioned in Sec. III A, in order to find the transition line, we use two kinds of procedures; one is given by linearized mean-field equation, while the other is determined by comparison of free energies of different states. In Fig. 3, we show calculated H-T phase diagram in magnetic field parallel to [001]. In the high-field region of the phase diagram, level crossing between Γ_6 and Γ_7 states is obtained in terms of larger magnitude and negative sign of g factor of the Γ_7 state. The transition at T_0 is of second order, and T_0 decreases with increasing magnetic field. The transition at T_1 is second-order transition from ferro-O_2^2 phase to coexistent phase of ferro-O_2^2 and antiferromagnetism. Here, the dashed line shows instability of paramagnetic state to ferro-O_2^2 state, while the dotted line is instability line of paramagnetic state to antiferromagnetic state with staggered moment parallel to [100]. The dashed line is very different from instability line shown in Fig. 1, since coupling constant between field induced $\phi^{\Gamma_4^-}$ is changed from ferrocoupling to antiferrocoupling. Comparing these instability lines with the transition line to the coexistent phase, ferro-O_2^2 and antiferromagnetism are cooperative to each other and stabilize the coexistent phase.
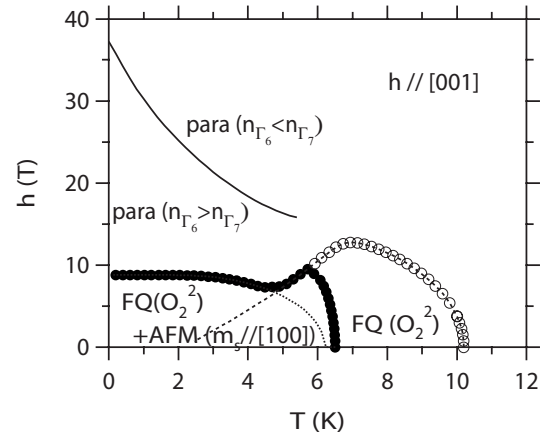
FIG. 3. h-T phase diagram in magnetic field parallel to [001]. The solid line shows level crossing temperature. The dashed and dotted lines are instability lines of disordered state to ferro-O_2^2 state and antiferromagnetic state with staggered moment parallel to [100], respectively. The open circle corresponds to transition point from disordered state to ferro-O_2^2 ordered state. The solid circle corresponds to transition point from paramagnetic state (including ferro-O_2^2 ordered state) to coexistent state of both ferro-O_2^2 moment and staggered magnetic moment parallel to [100]. These circles are determined by comparison of free energies.

In Fig. 4, we show calculated H-T phase diagram in magnetic field parallel to [100]. In this figure, T_0 is not a transition temperature but the crossover temperature from usual paramagnetic phase in high temperature region to disordered phase with considerable ferro-O_2^2 moment in low temperature region, where the crossover temperature is determined by inflection point of temperature dependence of C/T. The
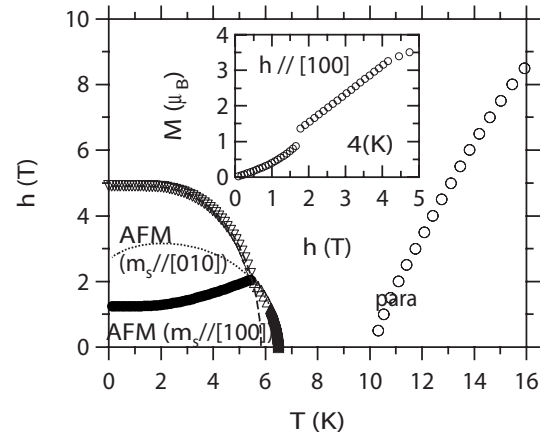
FIG. 4. h-T phase diagram in magnetic field parallel to [100]. The open circle shows crossover temperature determined by inflection point of temperature dependence of C/T. The dotted and dashed lines are instability lines of disordered state to antiferromagnetic state with staggered moment parallel to [100] and parallel to [010], respectively. The up triangle and down triangle correspond to transition point from disordered state to antiferromagnetic state with staggered moment parallel to [100] and parallel to [010], respectively, which are determined by comparison of free energies. Inset shows magnetization in field parallel to [100].

crossover temperature increases with increasing magnetic field. In order to consider low temperature state, we take into account reduced coupling constant between J^y, which is mentioned in Sec. IV. By the anisotropic magnetic interaction, we have two antiferromagnetic phases. Here, low-field phase has staggered moment parallel to the magnetic field, while high-field phase has perpendicular component to the magnetic field. Therefore, spin-flop transition is obtained, where the transition between these phases is of first order. If we use the same coupling constant as the one between J^x, low-field antiferromagnetic phase disappears. In the inset of Fig. 4, metamagnetic transition corresponding to the spin flop is obtained.

C. Specific heat

In specific heat data, there are some anomalous features in the temperature and field dependences. In magnetic field parallel to [001], specific heat jumps are observed at T_0 and T_1, and these transition temperatures decrease with increasing magnetic field. In magnetic field perpendicular to [001], the anomaly at the nonmagnetic transition reduces to a hump and broadens with increasing magnetic field. In order to compare with the experimental data, we calculate specific heat in magnetic field, based on the mean-field solution.

In order to calculate specific heat, we first provide expression of internal energy E_I, as follows:

$$E_I = \sum_{\mathbf{j}} \sum_n \epsilon_n \langle \psi_{\mathbf{j}n}^{\Gamma_1} \rangle - \sum_{\mathbf{i} \neq \mathbf{j}} \sum_{\Gamma, n} J_{\mathbf{i-j}n}^{\Gamma} \langle \psi_{\mathbf{i}n}^{\Gamma} \rangle \langle \psi_{\mathbf{j}n}^{\Gamma} \rangle, \quad (26)$$

where the first term of right hand side exhibits contributions from CEF term and Zeeman term. Then, specific heat is given by temperature derivative of the internal energy as

$$C = \sum_{\mathbf{j}} \sum_n \epsilon_n \frac{d\langle \psi_{\mathbf{j}n}^{\Gamma_1} \rangle}{dT} - \sum_{\mathbf{i} \neq \mathbf{j}} \sum_{\Gamma, n} 2 J_{\mathbf{i-j}n}^{\Gamma} \langle \psi_{\mathbf{i}n}^{\Gamma} \rangle \frac{d\langle \psi_{\mathbf{j}n}^{\Gamma} \rangle}{dT}, \quad (27)$$

with equation of temperature derivative of $\langle \psi_{\mathbf{j}n}^{\Gamma} \rangle$

$$\frac{d\langle \psi_{\mathbf{j}n}^{\Gamma} \rangle}{dT} = \sum_{n'} \frac{\epsilon_{n'}}{T} \chi_{\mathbf{j}n'n}^{\Gamma_1 \Gamma} - \sum_{\mathbf{i}(\neq \mathbf{j})} \sum_{\Gamma', n'} 2 J_{\mathbf{i-j}n'}^{\Gamma'}$$

$$\times \left(\frac{\langle \psi_{\mathbf{i}n'}^{\Gamma'} \rangle}{T} - \frac{d\langle \psi_{\mathbf{i}n'}^{\Gamma'} \rangle}{dT} \right) \chi_{\mathbf{j}n'n}^{\Gamma' \Gamma}. \quad (28)$$

where $\chi_{\mathbf{i}n'n}^{\Gamma' \Gamma}$ is given by the sublattice dependent expression

$$\chi_{\mathbf{i}n'n}^{\Gamma' \Gamma} = \int_0^{1/T} d\tau \langle \psi_{\mathbf{i}n'}^{\Gamma'}(\tau) \psi_{\mathbf{i}n}^{\Gamma} \rangle - \frac{\langle \psi_{\mathbf{i}n'}^{\Gamma'} \rangle \langle \psi_{\mathbf{i}n}^{\Gamma} \rangle}{T}. \quad (29)$$

Using these expressions, we calculate the specific heat of the system in a magnetic field. In Figs. 5(a) and 5(b), we show temperature dependences of specific heat for field parallel to [001] and [100] directions, respectively. In Fig. 5(a), there are two specific heat jumps corresponding to transitions to ferro-O_2^2 state at T_0 and to coexistent state at T_1. In addition, field dependence of the specific heat is very weak in low-field region. In Fig. 5(b), only specific heat jump is due to transition to antiferromagnetic state at T_1, while hump
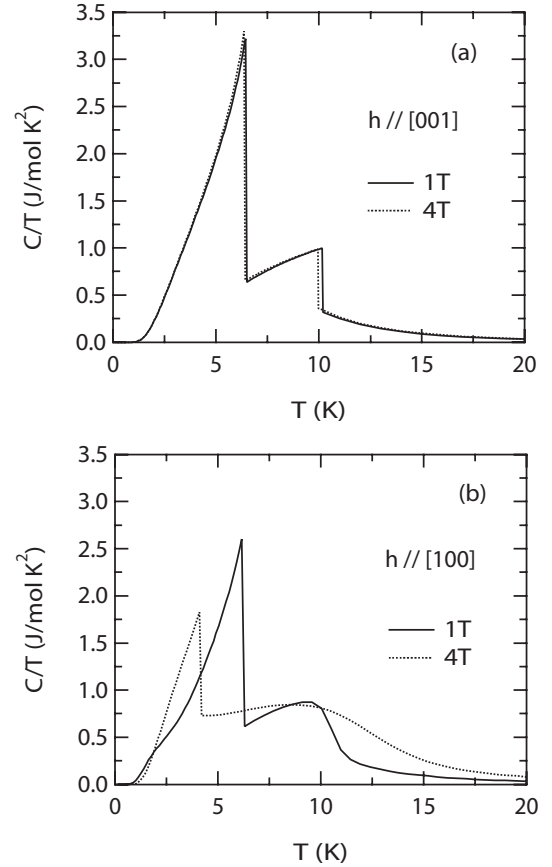
FIG. 5. Temperature dependences of specific heat in magnetic field parallel to [001] (a) and parallel to [100] (b). The solid and dotted lines correspond to 1 T and 4 T, respectively.

structure related to the crossover temperature at T_0 broadens with increasing magnetic field. This means that the ferro-O_2^2 moment is induced by magnetic field parallel to [100], as shown in Table III and no symmetry breaking at T_0 takes place for $H > 0$.

D. Uniform susceptibility

The experimental data of uniform susceptibility exhibit characteristic properties. In the magnetic field perpendicular to [001], uniform susceptibility does not show anomaly at T_0, except for the slight increase of magnitude of the temperature derivative at T_0 in low-field region. On the other hand, temperature dependence of uniform susceptibility in magnetic field parallel to [001] has a plateaulike behavior between T_0 and T_1. In addition, the temperature dependence is almost insensitive to the magnetic field up to 3 T. In order to analyze uniform susceptibility, we give expressions of the quantity in magnetic field parallel to [001] and [100]. For direct comparison with experimental data in finite magnetic field, magnetization divided by magnitude of the field is used as uniform susceptibility, instead of the Kubo formula of susceptibility from linear response theory. Then, uniform susceptibility χ_c in magnetic field parallel to [001] is given by
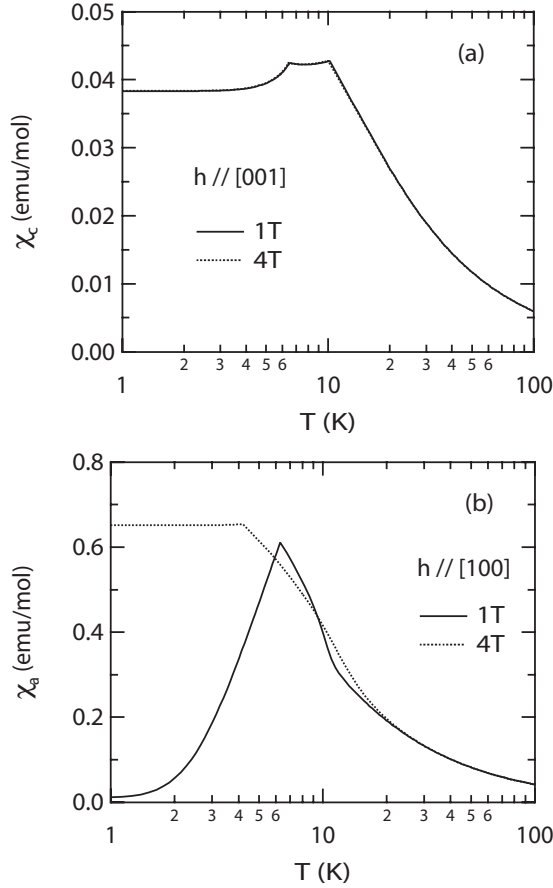
FIG. 6. Temperature dependences of uniform susceptibilities in magnetic field parallel to (a) [001] and (b) [100]. The solid and dotted lines correspond to 1 T and 4 T, respectively.

$$\chi_c = \frac{g_J\mu_B}{h}\langle J^z \rangle, \tag{30}$$

while uniform susceptibility in magnetic field parallel to [100] is similarly obtained from

$$\chi_a = \frac{g_J\mu_B}{h}\langle J^x \rangle, \tag{31}$$

where J^z and J^x are given by Eqs. (6) and (7), respectively.

In Fig. 6(a), we show calculated temperature dependence of uniform susceptibility in magnetic field parallel to [001]. Anomalies due to two transitions at T_0 and T_1 are obtained. Here, we note that plateau in temperature dependence between T_0 and T_1 is due to moderate coupling constant between octupoles $\phi^{\Gamma_4^-}$, which are induced by the magnetic field, while temperature independent behavior well below T_1 reflects existence of staggered moment perpendicular to the magnetic field. In addition, the uniform susceptibility hardly has field dependence at least in the low-field region. In Fig. 6(b), we show temperature dependence of uniform susceptibility in magnetic field parallel to [100]. From the figure, it shows slight upturn around crossover temperature T_0. In magnetic field of 1 T, it shows a cusp at transition temperature to antiferromagnetism with staggered moment parallel to

the magnetic field. With increase of magnetic field to 4 T, the uniform susceptibility shows temperature independent behavior below transition temperature to antiferromagnetism with staggered moment perpendicular to the magnetic field. The difference of behavior below antiferromagnetic transition temperature is due to the spin-flop transition, as shown in Fig. 4.

VI. DISCUSSION AND SUMMARY

Before we summarize, we would like to comment on a few points. In the previous section, we have calculated specific heat, uniform susceptibility, and phase diagram with assumption of ferro-O_2^2 ordering at T_0. Comparing our results with experimental data of YbRu$_2$Ge$_2$, the present model not only explains the experimental data qualitatively, but also gives quantitative agreement in specific heat jumps. Therefore, ferro-O_2^2 ordering at T_0 above antiferromagnetic transition temperature T_1 will be one of promising candidate for nonmagnetic transition of YbRu$_2$Ge$_2$. However, we have proposed either ferro-O_2^2 or ferro-O_{xy} ordering for the transition at T_0 in Sec. III. Considering that both candidates are ferro-ordering states of quadrupoles, in order to identify the nonmagnetic state among the two candidates, it will be useful to carry out ultrasonic and x-ray scattering experiments, because ferroquadrupole couples with lattice distortion. From this point of view, it is desirable to confirm the crystal structure below T_0.

Related to property of nonmagnetic ordering state, it has been recently reported that Ru-NQR spectrum may not be affected by the nonmagnetic transition.[18] With respect to this result, taking into account positions of Yb and Ru ions, if dominant quadrupole of Ru nucleus is either O_2^0 or O_2^2, ferro-O_{xy} ordering of Yb^{3+} does not change Ru-NQR spectrum by the transition. On the other hand, if quadrupole of Ru nucleus is O_{xy}, ferro-O_2^2 ordering does not change the spectrum by the transition. Furthermore, if quadrupole of Ru nucleus is either O_{yz} or O_{zx}, both ferro-O_2^2 ordering and ferro-O_{xy} ordering do not change the spectrum. In order to identify the type of quadrupole ordering, it is required to clarify the quadrupole of Ru nucleus.

Furthermore, in recent uniform susceptibility data, it is shown that behavior of uniform susceptibility in magnetic field parallel to [100] is similar as that in magnetic field parallel to [110], and these uniform susceptibilities have finite value at very low temperature. Based on the present model with assumption of either ferro-O_2^2 or ferro-O_{xy} ordering at T_0, one of these uniform susceptibility will vanish at 0 K in small magnetic field region by development of staggered magnetic moment parallel to the magnetic field. Considering that finite values are observed for both uniform susceptibilities in very low temperature region, the ordering wave vector of magnetic moments will be an incommensurate one. Therefore, it is desirable to carry out neutron scattering experiment to clarify the magnetic state of the compound.

Finally, we comment on effect of multipolar fluctuations. The effect has been investigated in CeB$_6$ by Shiina.[19] In this paper, it has been shown that the multipolar fluctuation are

enhanced by approaching the system to the $SU(4)$ symmetric limit. In YbRu$_2$Ge$_2$, it is considered that the tetragonal anisotropy such as splitting energy Δ between Γ_6 and Γ_7 states breaks the $SU(4)$ symmetry inherently. Therefore, we do not expect that the multipolar fluctuations change qualitatively behaviors suggested by the mean-field theory.

In summary, in order to explain properties of YbRu$_2$Ge$_2$, we have introduced a quasidegenerate localized model consisting of CEF term, Zeeman term, and exchange term of multipoles. Classifying multipoles according to irreducible representations of corresponding point group, we have developed a mean-field theory for the model. Considering that the specific heat jump broadens with increasing magnetic field perpendicular to [001], we have proposed that for the nonmagnetic transition, only ferro-O_2^2 and ferro-O_{xy} orderings are possible candidates. Furthermore, it has been shown that these ferro-quadrupole orderings are only available and essentially of the induced type, when the lower two CEF states consist of one Γ_6 and one Γ_7 doublets in zero magnetic field. With assumption of ferro-O_2^2 ordering at T_0, we have calculated specific heat, uniform susceptibility, and phase diagram, where anisotropic exchange interaction between planar components of magnetic moments is introduced as an effect of the ferroquadrupole ordering. The calculated results have been shown to explain experimental data consistently. In order to clarify the property of YbRu$_2$Ge$_2$ completely and refine the set of coupling constants, it is desirable to carry out more detailed experiments such as elastic constant measurements and neutron diffraction in applied magnetic field.

[1] T. Fujita, M. Suzuki, T. Komatsubara, S. Kunii, T. Kasuya, and T. Ohtsuka, J. Phys. Soc. Jpn. **35**, 569 (1980).

[2] M. Takigawa, H. Yasuoka, T. Tanaka, and Y. Ishizawa, J. Phys. Soc. Jpn. **52**, 728 (1983).

[3] J. M. Effantin, J. Rossat-Mignod, P. Burlet, H. Bartholin, S. Kunii, and T. Kasuya, J. Magn. Magn. Mater. **47&48**, 145 (1985).

[4] D. Mannix, G. H. Lander, J. Rebizant, R. Caciuffo, N. Bernhoeft, E. Lidström, and C. Vettier, Phys. Rev. B **60**, 15187 (1999).

[5] J. A. Paixão, C. Detlefs, M. J. Longfield, R. Caciuffo, P. Santini, N. Bernhoeft, J. Rebizant, and G. H. Lander, Phys. Rev. Lett. **89**, 187202 (2002).

[6] S. W. Lovesey, E. Balcar, C. Detlefs, G. van der Laan, D. S. Sivia, and U. Staub, J. Phys.: Condens. Matter **15**, 4511 (2003).

[7] Y. Tokunaga, Y. Homma, S. Kambe, D. Aoki, H. Sakai, E. Yamamoto, A. Nakamura, Y. Shiokawa, R. E. Walstedt, and H. Yasuoka, Phys. Rev. Lett. **94**, 137209 (2005).

[8] J. W. Ross and D. J. Lam, J. Appl. Phys. **38**, 1451 (1967).

[9] P. Erdös, G. Solt, Z. Zolnierek, A. Blaise, and J. M. Fournier, Physica B & C **102B**, 164 (1980).

[10] H. S. Jeevan, C. Geibel, and Z. Hossain, Phys. Rev. B **73**, 020407(R) (2006).

[11] R. Shiina, H. Shiba, and P. Thalmeier, J. Phys. Soc. Jpn. **66**, 1741 (1997).

[12] R. Shiina, H. Shiba, and O. Sakai, J. Phys. Soc. Jpn. **68**, 2105 (1999).

[13] K. Kubo and T. Hotta, Phys. Rev. B **71**, 140404(R) (2005).

[14] G. T. Trammell, J. Appl. Phys. **31**, 362S (1960); Phys. Rev. **131**, 932 (1963).

[15] B. Bleaney, Proc. R. Soc. London, Ser. A **276**, 19 (1963).

[16] C. Geibel (private communication).

[17] In Fig. 1(a), we can see the sign of the level cross around 20 T. Here, we should note that this first-order transition is different from nonmagnetic transition observed in YbRu$_2$Ge$_2$, because this transition is not expected in low-field region.

[18] H. Mukuda (private communication).

[19] R. Shiina, J. Phys. Soc. Jpn. **70**, 2746 (2001).